Photosynth Res (2007) 94:347–357
DOI 10.1007/s11120-006-9127-z

REGULAR PAPER

Quantification of cyclic electron flow around Photosystem I in spinach leaves during photosynthetic induction

Da-Yong Fan · Qin Nie · Alexander B. Hope · Warwick Hillier · Barry J. Pogson · Wah Soon Chow

Received: 31 August 2006 / Accepted: 11 December 2006 / Published online: 9 January 2007

Abstract The variation of the rate of cyclic electron transport around Photosystem I (PS I) during photosynthetic induction was investigated by illuminating dark-adapted spinach leaf discs with red + far-red actinic light for a varied duration, followed by abruptly turning off the light. The post-illumination re-reduction kinetics of $P700^+$, the oxidized form of the photoactive chlorophyll of the reaction centre of PS I (normalized to the total P700 content), was well described by the sum of three negative exponential terms. The analysis gave a light-induced total electron flux from which the linear electron flux through PS II and PS I could be subtracted, yielding a cyclic electron flux. Our results show that the cyclic electron flux was small in the very early phase of photosynthetic induction, rose to a maximum at about 30 s of illumination, and declined subsequently to <10% of the total electron flux in the steady state. Further, this cyclic electron flow, largely responsible for the fast and intermediate exponential decays, was sensitive to 3-(3,4-dichlorophenyl)-1,1-dimethyl urea, suggesting an important role of redox poising of the cyclic components for optimal function. Significantly, our results demonstrate that analysis of the post-illumination re-reduction kinetics of $P700^+$ allows the quantification of the cyclic electron flux in intact leaves by a relatively straightforward method.

D.-Y. Fan
Laboratory of Quantitative Vegetation Ecology, Institute of Botany, The Chinese Academy of Sciences, Beijing 100093, China

D.-Y. Fan · Q. Nie · W. Hillier · W. S. Chow (✉)
Photobioenergetics Group, Research School of Biological Sciences, The Australian National University, Canberra, ACT 0200, Australia
e-mail: chow@rsbs.anu.edu.au

A. B. Hope
Faculty of Science and Engineering, School of Biological Sciences, Flinders University, GPO Box 2100, Adelaide, SA 5001, Australia

B. J. Pogson
School of Biochemistry and Molecular Biology, The Australian National University, Canberra, ACT 0200, Australia

Present Address:
Q. Nie
College of Resources and Planning Sciences, Jishou University, Jishou, Hunan Province 427000, China

Keywords Cyclic electron transport · P700 · Photosynthetic induction · Photosystem I

Abbreviations

ATP	Adenosine triphosphate
Chl	Chlorophyll
DCMU	3-(3,4-Dichlorophenyl)-1, 1-dimethyl urea
Fd	Ferredoxin
F_v' and F_m'	Variable and maximum Chl fluorescence during illumination
MV	Methyl viologen
$NADP^+$	Oxidized nicotinamide adenine dinucleotide phosphate
P700	Photoactive Chl of the reaction centre of PS I
PS I and PS II	Photosystem I and II, respectively
PQ	Plastoquinone

Introduction

Arnon et al. (1955) demonstrated that ATP synthesis is induced by illumination of thylakoids in the presence of vitamin K through a pathway of cyclic electron transport around Photosystem I (PS I). Since then, great efforts have been made to understand the physiological significance of this cyclic pathway. Although current evidence supports an important role for cyclic electron transport in C4 photosynthesis (Herbert et al. 1990; Furbank et al. 1990), the evidence for and against cyclic electron transport as a significant process in C3 plants (reviewed by Bendall and Manasse 1995; Allen 2003; Buhkov and Carpentier 2004; Johnson 2005; Joliot and Joliot 2006) under normal steady-state physiological conditions requires further investigation. A strong piece of evidence for an important role of cyclic electron transport in steady-state conditions is in a recent report of an *Arabidopsis* mutant that is incapable of cyclic electron transport and, consequently, severely impaired in growth and development (Munekage et al. 2004). However, to our knowledge, quantification of the cyclic electron flux in this mutant in comparison with the wild type has yet to be made.

In terms of chloroplast energetics, if the current view about the H^+/e^- ratio of 3 and the H^+/ATP ratio of 4.7 is correct (Allen 2003), only 2.55 ATP molecules are synthesized per O_2 molecule released, which means an additional half an ATP molecule needs to be generated via cyclic electron transport for the fixation of each CO_2 molecule, or via the Mehler-ascorbate-peroxidase cycle. Furthermore, the modulation of the ATP:NADPH ratio and the generation of a *trans*-thylakoid pH gradient via cyclic electron transport may facilitate a flexible response of leaves to changing environmental conditions (Kramer et al. 2004). Thus, as demand for ATP increases relative to that for NADPH, cyclic electron flow is increased, as supported by studies during the photosynthetic induction period (Joliot and Joliot 2002, 2005, 2006), at elevated temperatures (Havaux 1996; Buhkov et al. 1999; Clarke and Johnson 2001), at chilling temperatures (Clarke and Johnson 2001), under anaerobiosis (Joët et al. 2002) and under drought (Golding et al. 2004).

Primarily based on an analysis of the onset kinetics of P700 photo-oxidation in dark-adapted leaves on illumination with far-red light (Joliot and Joliot 2005, 2006), or the decay of 515 nm absorption during short interruptions in illumination (Joliot and Joliot 2002), it was concluded that there is a substantial initial rate of cyclic electron transport on illumination of dark-adapted leaves, and that pre-illumination induces a transition from the cyclic to the linear mode. Measurements of the decay of oxidized P700 following brief (up to 1 s) light flashes given to dark-adapted leaves also support the transient cyclic electron flow in previously dark-adapted leaves (Golding et al. 2004) though no fluxes as such were presented. Similarly, the changing of cyclic electron transport as a fraction of the total during illumination is also indicated by a decrease of F_v'/F_m' (the quantum efficiency of open PS II reaction centres) from 0.76 at beginning to 0.64 after 5 min far-red illumination at 1°C (Cornic et al. 2000).

Unfortunately, quantification of the cyclic electron flux during photosynthetic induction has not been straightforward. For example, the method based on the onset kinetics of P700 oxidation in dark-adapted leaves is complicated by the extreme variability (Joliot and Joliot 2005). Therefore, we sought an alternative method that analyses the decay of the $P700^+$ signal after illumination (Maxwell and Biggins 1976), and from which the electron flux to $P700^+$ can be deduced (Chow and Hope 2004). To the extent that we cannot separate charge recombination, if it occurred, from energy-conserving cyclic electron flux via the PQ pool and PS I, the cyclic electron flux that we obtained may include a dissipative charge-recombination component.

In this paper, we evaluated the electron transport flux to $P700^+$ by fitting, with the sum of three negative exponential components, the $P700^+$ re-reduction kinetics on cessation of red + far-red illumination. We quantified the relative fraction of cyclic electron flow during illumination of dark-adapted spinach leaves, and showed that red + far-red illumination of dark-adapted leaves gave rise to dynamic changes in cyclic electron transport during photosynthetic induction. We also investigated the relationship between cyclic electron flow and redox poise of electron carriers between the two photosystems, showing that DCMU inhibited not only the MV-resistant fast linear electron flux to $P700^+$, but also the MV-sensitive fast electron flux which is attributable to cyclic electron flow.

Materials and methods

Spinacia oleracea L. cv. Yates hybrid 102 plants were grown at 24/21°C (day/night) with a 10-h photoperiod (230 μmol photons m^{-2} s^{-1}). The potting mixture was supplemented by a slow release fertilizer ('Osmocote', Scotts Australia Pty Ltd., Castle Hill).

Post-illumination re-reduction kinetics of $P700^+$

Redox changes of P700 in spinach leaf discs were observed with a dual wavelength (820/870 nm) unit (ED-P700DW) attached to a phase amplitude modulation fluorometer (Walz, Effeltrich, Germany) that was used in the reflectance mode (Chow and Hope 2004). To obtain the maximum signal corresponding to the total amount of photo-oxidizable P700 ($P700^+_{max}$), a steady-state was first sought by illumination with far-red light (12 μmol photons m^{-2} s^{-1}, peak wavelength 723 nm, 102-FR, Walz, Effeltrich, Germany) for ≥10 s. Then a single-turnover xenon flash (XST 103 xenon flash) was applied to the adaxial side of the leaf disc. Flashes were given at 0.1 Hz, and 16 consecutive signals were averaged (time constant = 95 μs). The maximum signal amplitude immediately after the flash was taken as the total amount of photo-oxidizable P700, and used to normalize the signals obtained in the same geometry with a stronger red + far-red actinic light (see below).

To measure the re-reduction kinetics of $P700^+$ on cessation of illumination with red + far-red actinic light, leaf discs were first vacuum infiltrated with either H_2O, methyl viologen (MV, 300 μM) or DCMU (100 μM, unless stated otherwise), blotted with absorbent paper, and allowed to evaporate off the excess intercellular water, and then kept in a humidified container for a total of 1-h darkness before measurement. Red + far-red actinic light from a slide projector was selected by an RG 695 long-pass filter combined with a Calflex C heat-reflection filter. The direction of the actinic light made an angle of ca. 60° with the horizontal leaf disc, while the light guide also made an angle of ca. 60° but was on the opposite side of the vertical. The spectral irradiance measured by an LI1800 spectroradiometer (Licor, USA) is shown in Fig. 1, the irradiance being ca. 260 μmol photons m^{-2} s^{-1} (675–750 nm). Red + far-red actinic light was turned on by an electronic shutter triggered by a pulse/delay generator (Model 555, Berkeley Nucleonics Corporation, USA) for a required time interval and then turned off, while another pulse from the signal generator triggered a computer program to begin data acquisition (time constant = 2.3 ms) at 0.1 s before the actinic light was turned off; data acquisition continued into the dark period for 0.9 s. Signals from four to six separate leaf discs were averaged. The duration of illumination given to dark-adapted leaf discs was varied to investigate variation of the electron fluxes to $P700^+$ during photosynthetic induction.

The longest possible duration of actinic illumination controlled by the signal generator was 90 s. To extend the duration of illumination, we repeatedly illuminated leaf discs with bursts of actinic light, each of duration 2 s, and periodically stored the data for the post-illumination re-reduction kinetics of $P700^+$. In this way we were able to investigate cumulative periods of photosynthetic induction up to 10 min.

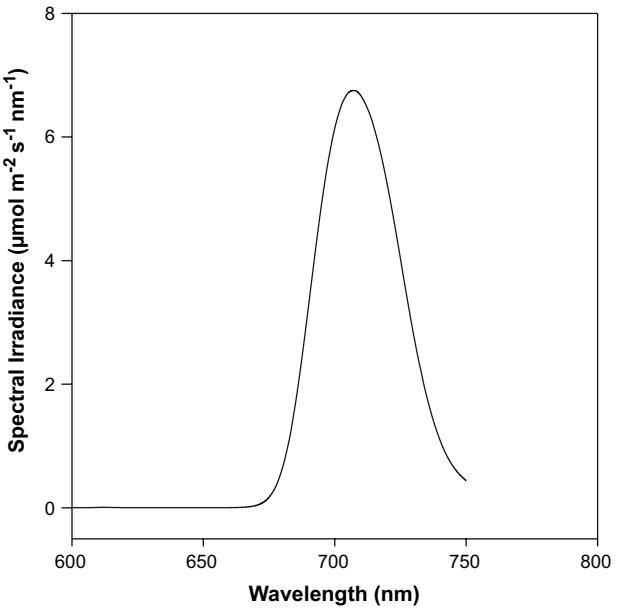

Fig. 1 Spectral distribution of the red + far-red actinic light. The red irradiance (≤700 nm) was 70 μmol photons m^{-2} s^{-1}, while the far-red irradiance (701–750 nm) was 190 μmol photons m^{-2} s^{-1}

All post-illumination $P700^+$ signals were normalized to $P700^+_{max}$ obtained in the same geometry (described earlier) to give the fraction of oxidized P700 at any instant. During illumination, the concentration of $P700^+$ was determined by the rate of photo-oxidation counteracted by re-reduction by electrons from various sources. On abruptly turning off the actinic light, photo-oxidation ceased immediately, but the re-reduction continued for some time. The initial rate of re-reduction of $P700^+$, therefore, should be equal to the electron flux to $P700^+$ immediately before cessation of illumination. Hence, our objective was to determine the initial rate of re-reduction of $P700^+$ on abruptly turning off the red + far-red actinic light. The re-reduction kinetics (Fig. 2) were well fitted by the sum of three negative exponentials, with normalized amplitudes A_1, A_2 and A_3, and rate coefficients k_1, k_2 and k_3, yielding the total initial rate of re-reduction of $P700^+$ (hereafter termed "total electron flux") $A_1k_1 + A_2k_2 + A_2k_2$, in turnovers of each P700 per second.

The rate of electron transport through PS II measured by Chl *a* fluorescence

The relative Chl *a* fluorescence yield (F) at any instant during photosynthetic induction and the maximum

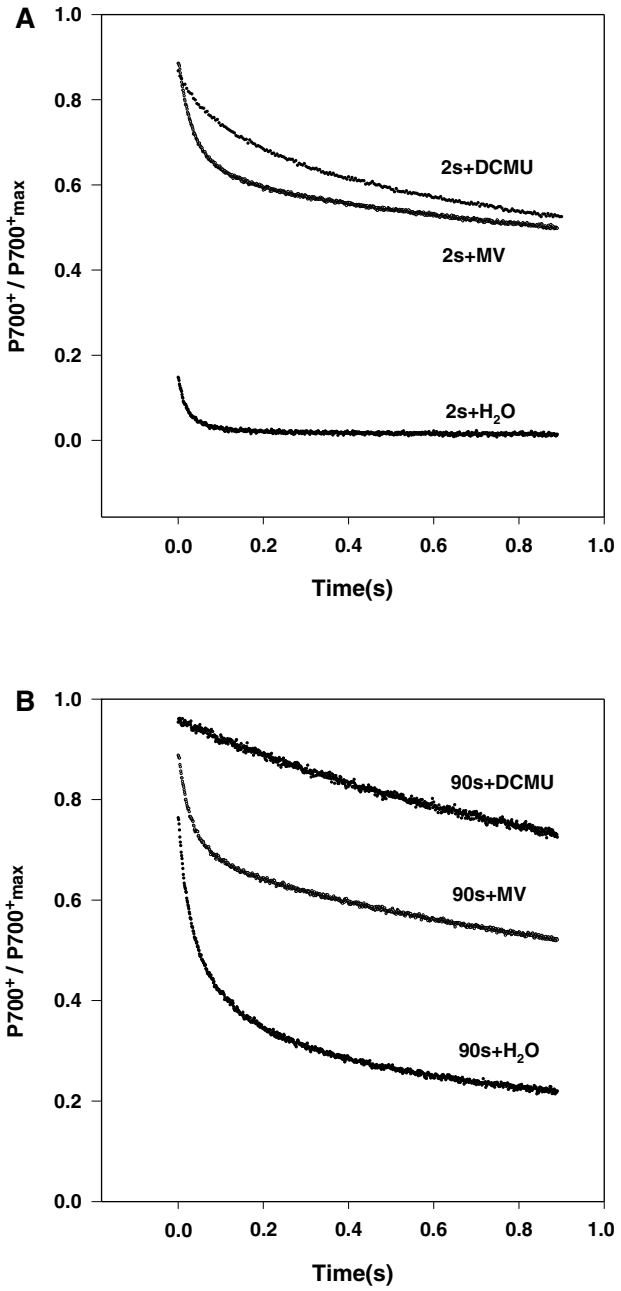

Fig. 2 The re-reduction kinetics of $P700^+$ in spinach leaf discs on cessation of illumination with red + far-red actinic light. Red + far-red light (ca. 260 μmol photons m^{-2} s^{-1}) was turned on by an electronic shutter for 2 s (**A**) or 90 s (**B**), then turned off at time $t = 0$. The decay signal was recorded for 0.9 s. Each trace is the average for four leaf discs. Leaf discs were cut from spinach plants in a growth chamber during the photoperiod, infiltrated in darkness with water, 100 μM DCMU or 300 μM MV (all with 0.5% ethanol, v/v) and allowed to evaporate off excess intercellular water in darkness for 40 min. Afterwards, leaf discs were put on wet filter paper for a further 20 min darkness (total dark time = 60 min) before red + far-red light was given. Further details are described in the "Materials and methods" section

relative Chl *a* fluorescence yield at the same instant (F_m') were measured. The Chl *a* fluorescence yield, induced by blue modulated light, was measured at wavelengths >660 nm, with little or no contamination by PS I fluorescence. The average quantum yield of PS II photochemistry, averaged over open and closed PS II reaction centre traps, is given by $1 - F/F_m'$ (Genty et al. 1989). This quantity can be used to calculate the rate of electron transport through PS II (ETR, Schreiber 2004) as $(1 - F/F_m') \times I \times A \times f$ where I is the irradiance, A the absorptance of the leaf and f is the fraction of absorbed light partitioned to PS II. Since ETR is directly proportional to $(1 - F/F_m')$, we used this quantity as a relative measure of the rate of linear electron transport during photosynthetic induction. Leaf discs infiltrated with H_2O (control) or MV were used after evaporation of excess intercellular water and dark-adaptation for a total of 1 h.

Results

Post-illumination re-reduction kinetics of $P700^+$ for quantifying the electron flux to $P700^+$

Illumination of dark-adapted spinach leaf discs with red + far-red actinic light led to a time-dependent extent of net photo-oxidation of P700, while cessation of illumination resulted in re-reduction of $P700^+$. In control leaves infiltrated with water, 2 s red + far-red illumination gave a limited extent of photo-oxidation, which rapidly relaxed in the post-illumination period (Fig. 2A). On the other hand, the presence of either DCMU (to inhibit PS II) or MV (to promote electron flow from PS I to O_2) resulted in 90% of P700 being photo-oxidized even after just 2 s; re-reduction in darkness was comparatively slow (Fig. 2A). At 90-s illumination, >75% of the P700 was photo-oxidized even in a control sample pre-infiltrated with H_2O (Fig. 2B).

The re-reduction kinetics of $P700^+$ were fitted as the sum of three negative exponentials (slow, intermediate and fast), yielding rate coefficients which, when multiplied by the respective amplitudes, gave the initial fluxes. Both the rate coefficients and the fluxes are shown as a function of duration of illumination of dark-adapted leaf discs (Fig. 3). There was an order of magnitude difference between slow and intermediate, and between intermediate and fast rate coefficients (Fig. 3A–C). Similarly, successive initial fluxes also differ by an order of magnitude (Fig. 3D–F). The total initial flux (Fig. 3G) in H_2O-infiltrated samples (solid circle), equated with the total rate of electron flow to $P700^+$ at

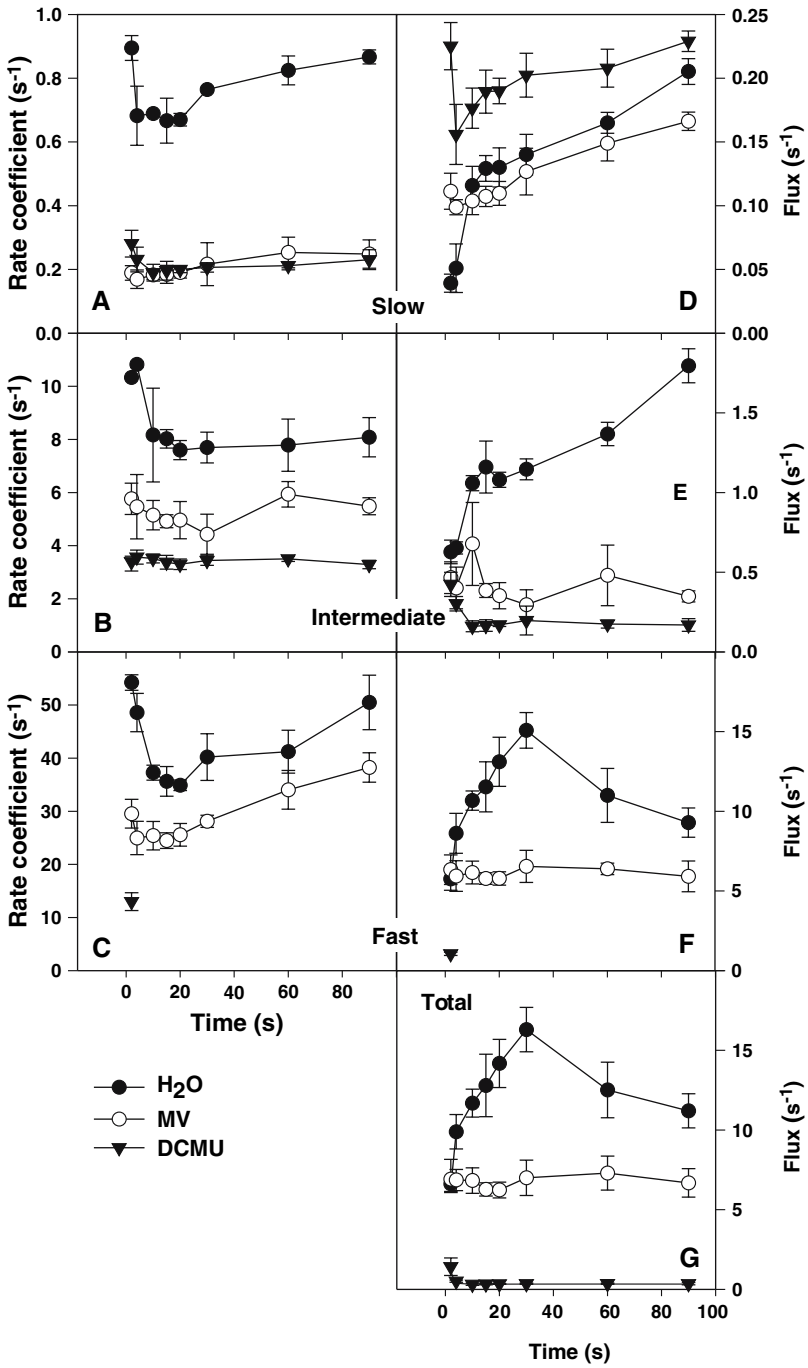

Fig. 3 Rate coefficients (s^{-1}) and the fluxes (turnovers of each P700 s^{-1}) of slow, intermediate and fast components derived from the sum of three negative exponentials of best fit to the post-illumination kinetics of $P700^+$ re-reduction. The *x*-axis shows the time of illumination (from 2 to 90 s) before the actinic light was turned off. Results are the average of six experiments using leaf discs infiltrated with water (●), 300 μM MV (○) or 100 μM DCMU (▼). Total flux = slow flux + intermediate flux + fast flux. Other conditions as for Fig. 2

the instant the actinic light was turned off, increased with time of illumination, reaching a peak at about 30 s of illumination. In the presence of MV (open circles), the total flux was relatively constant, while in the presence of DCMU (inverted triangles), the flux declined to a small value within 4 s of illumination (Fig. 3G).

Estimation of the linear electron flux

MV was expected to rapidly shunt electrons to oxygen and abolish any cyclic electron flow, leaving only linear electron flow. However, the difference in total fluxes between H_2O- and MV-infiltration cannot be directly equated with the cyclic electron flux. This is because photosynthetic induction manifested itself in H_2O-infiltrated samples but not in MV-infiltrated samples. Therefore, to estimate the linear electron flux in the presence of photosynthetic induction, we measured the quantum yield of PS II photochemistry during illumination ($1 - F/F_m'$), averaged over open and closed PS II reaction centre traps (Genty et al. 1989). This parameter is directly proportional to the rate of

electron transport through PS II (Schreiber 2004). Figure 4 shows the variation of $(1 - F/F_m')$ during photosynthetic induction, in leaves that had been infiltrated with either H_2O or MV. In the absence of MV, there was a slight decrease in $(1 - F/F_m')$ at 15–30 s of illumination, but an increase at 60–90 s. Interestingly, $(1 - F/F_m')$ was the same between MV and H_2O infiltration after 60–90 s of photosynthetic induction. That is, the linear electron flux was the same whether or not MV was present, provided sufficient photosynthetic induction time had lapsed.

Estimation of the cyclic electron flux

We took advantage of this latter observation of the same $(1 - F/F_m')$ for MV- and H_2O-infiltration after 60–90 s, so as to evaluate the cyclic electron flux during photosynthetic induction. By scaling $(1 - F/F_m')$ for H_2O-infiltrated samples in Fig. 4 to assume the same flux value at 60 s as for MV-infiltrated samples in Fig. 3G (open circles, middle curve), we could estimate the linear flux, which is now plotted as curve (b) in Fig. 5A. Subtracting curve (b) from curve (c) (total flux, from the top curve of Fig. 3G) gave curve (a), the estimated cyclic electron flux (Fig. 5A). Both cyclic and linear electron fluxes are plotted in Fig. 5B, as a percentage of their sum. It is clear that the linear

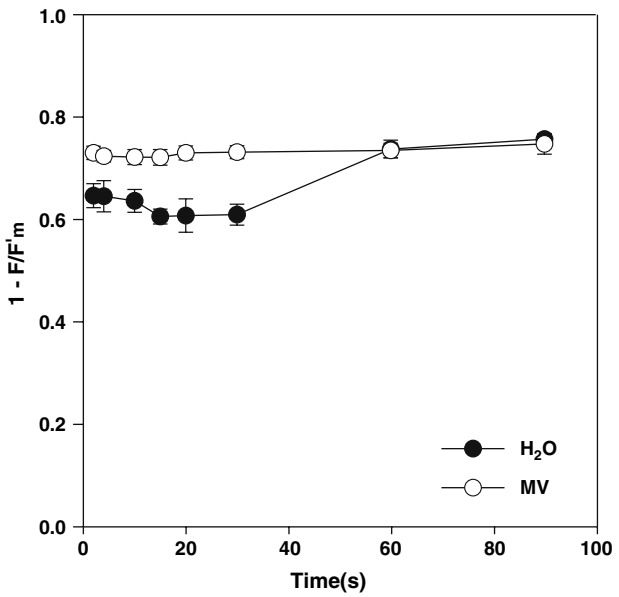

Fig. 4 Changes in the average quantum yield of PS II $(1 - F/F_m')$ as a function of photosynthetic induction time, when dark-adapted spinach leaf discs were illuminated with red + far-red actinic light. The dark time before each measurement was at least 60 min. Each point is an average of five replicates (±SD)

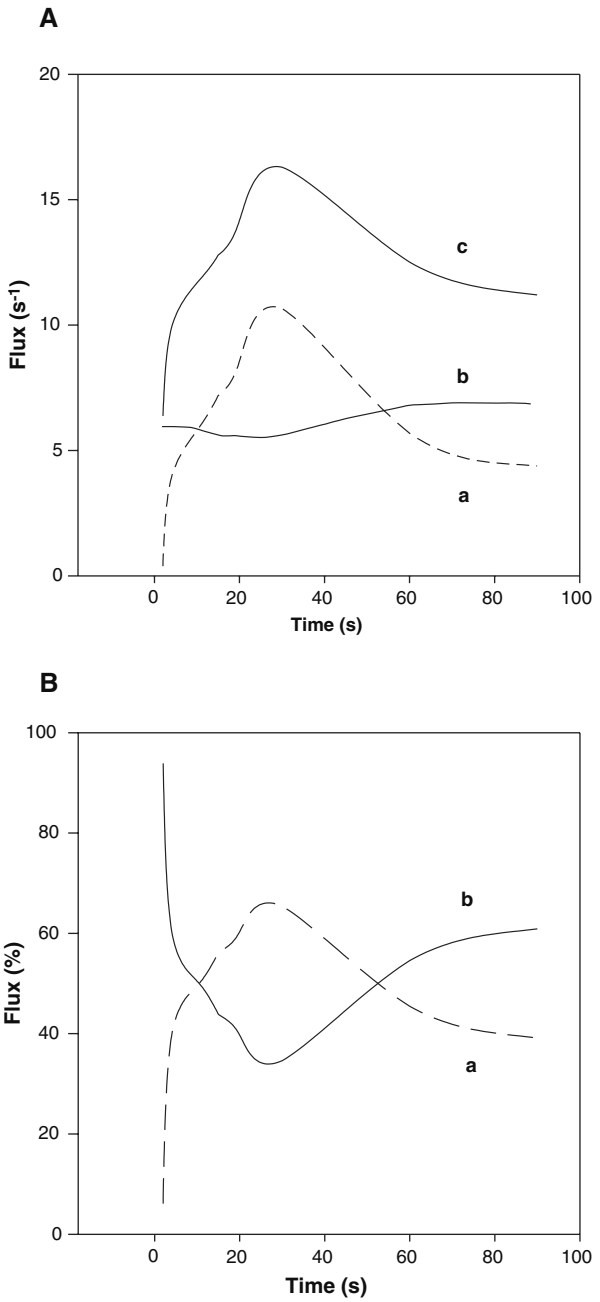

Fig. 5 Cyclic electron flux (curve (a)) and linear electron flux (curve (b)), as well as their sum (curve (c)), plotted as the original value (**A**) or as a percentage of the total electron flux (**B**) of dark-adapted spinach leaf discs subjected to illumination with red + far-red light. Curve (c) in panel A was taken from the H_2O-infiltrated control in Fig. 3G (top curve). Curve (b) in panel A was taken from the H_2O-infiltrated control in Fig. 4, scaled to assume the same flux value as the total flux for MV-infiltrated samples at 60-s illumination in Fig. 3G (middle curve). The rationale for this re-scaling is based on the observations that (i) $(1 - F/F_m')_{H2O} = (1 - F/F_m')_{MV}$ at 60 s (Fig. 4) and (ii) the rate of linear electron transport through PS II is directly proportional to $(1 - F/F_m')$

electron flux dominated at 2 s, decreasing rapidly to a minimum at ca. 30 s and then recovering by 90 s. The cyclic electron flux was small at 2 s, but peaked at about 68% at 30 s, declining thereafter. At 90 s, about 37% of the total was cyclic electron flux.

Our existing signal generator did not allow us to maintain the electronic shutter open for more than 90 s. To examine longer durations of illumination, we resorted to cumulative illumination with 2-s flashes, separated by 1.2 s dark time during which the post-flash kinetics could be recorded if required. Figure 6 shows (in a log-scale for time) that H_2O-infiltrated samples exhibited a maximum total electron flux after 30-s cumulative illumination, but that the difference between MV- and H_2O-infiltration was very small (~8%) after 600-s cumulative illumination.

The effect of DCMU on the cyclic electron flux

To investigate the action of DCMU on the electron fluxes in detail, we varied the concentration of DCMU in dark-adapted leaf discs that were all subjected (without interruption) to 30-s illumination with red + far-red light. This duration of illumination was chosen to maximize the cyclic electron flux. Notably, the greatest proportional decrease due to DCMU was in the fast flux, regardless of the absence (solid circles) or presence (open circles) of MV; at 35 μM DCMU, the fast flux was practically zero (Fig. 7F). The total flux is shown in Fig. 7G. In the presence of MV, the rate of linear electron flow was 20% greater than that which occurred under conditions of photosynthetic induction (30-s illumination, Fig. 4). Therefore, we think that the true linear flux, allowing for an effect of photosynthetic induction, is indicated by the dashed line in Fig. 7G. The difference between the total electron flux (solid line) and the true linear flux (dashed line) then gives the cyclic flux that was inhibited by DCMU. Since the bulk of the total flux was contributed by the fast flux and was MV-sensitive, it implies that, at 30-s illumination, a substantial part of the fast flux was indeed cyclic electron flow.

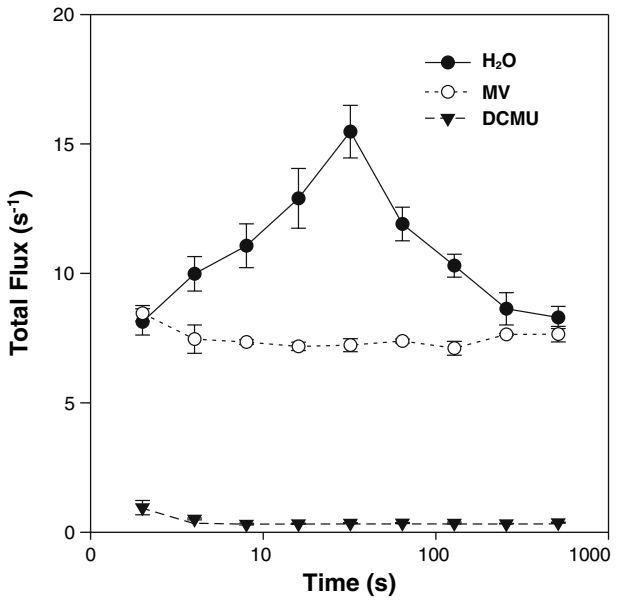

Fig. 6 The average total electron flux (±SEM) from six experiments using leaf discs infiltrated with water, 300 μM MV or 100 μM DCMU as a function of cumulative time of illumination with red + far-red actinic light (from 2 to 600 s). Dark-adapted leaf discs were subjected to cycles of 2 s red + far-red actinic light, 1.2 s darkness (the re-reduction kinetics of $P700^+$ were recorded during the 1.2 s darkness when required). [Ethanol] = 0.5%

The combined effect of DCMU and MV on the total electron flux

At 2-s illumination in the presence of DCMU, a small flux of ca. 0.8 turnovers of each P700 s^{-1} could be observed (Fig. 3G). To elucidate the contributions to this flux, we investigated the electron flux using DCMU and MV separately or in combination, exposing dark-treated leaves of another batch of plants to 2 s red + far-red light (Fig. 8). In the presence of MV alone, the flux was higher than that in H_2O-infiltrated samples, owing to the absence of photosynthetic induction. Interestingly, in the combined presence of DCMU and MV (i.e. in the absence of linear and cyclic electron flow), the total electron flux was 0.77 s^{-1}, as compared with 0.84 s^{-1} in the presence of DCMU alone. This residual electron flux of 0.77 s^{-1} at 2-s illumination represents electron donation to the inter-system electron transport chain other than via linear or cyclic electron flow. Its value decreased to 0.31 s^{-1} at 90-s illumination time (data not shown).

Discussion

The method of dark relaxation kinetics of $P700^+$ on cessation of illumination

Our method analyses the post-illumination re-reduction kinetics of $P700^+$ to obtain the rate of electron flow during illumination immediately before cessation of illumination. It is essentially equivalent to the dark-interval relaxation kinetics (DIRK) analysis of Sacksteder and Kramer (2000) in which the initial rate of relaxation of a steady-state absorbance signal is measured upon a light-to-dark transition. In our application of this method, however, the leaves did

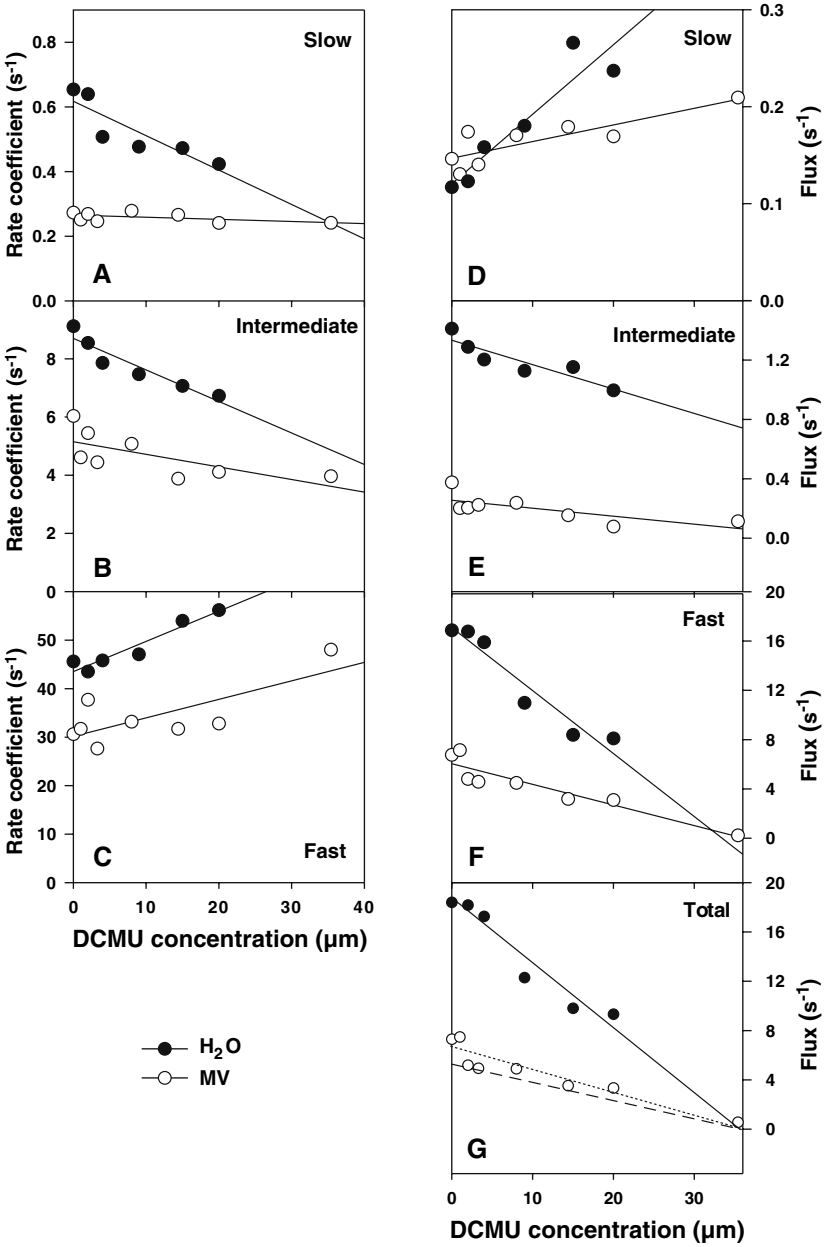

Fig. 7 The average rate coefficients and the average slow, intermediate and fast fluxes as a function of DCMU concentration (illumination time = 30 s) from two experiments using leaf discs infiltrated with DCMU of varied concentration either with (○) or without (●) 300 µM MV. The decay of $P700^+$ was recorded on cessation of illumination of leaf discs with red + far-red actinic light for 30 s. Other conditions as for Fig. 2

not achieve a steady state before measurement, because we were interested in the variation of electron fluxes during photosynthetic induction. Nevertheless, it appears valid to apply the method to a non-steady-state situation since the rate of photo-oxidation of P700 and the rate of re-reduction of $P700^+$ together determine the net rate of change of $[P700^+]$ at a given instant during illumination. Upon turning off actinic light abruptly, photo-oxidation ceases immediately, leaving re-reduction to occur with an initial rate equal to that just prior to cessation of illumination. Golding et al. (2005) pointed out that it should be possible to use the relaxation kinetics of $P700^+$ to estimate the electron flux through the reaction centre, provided that P700 is more than about 20% oxidized in the light. With this constraint in mind, we would expect that our estimation of the total flux to $P700^+$ to be valid for 4 s photosynthetic induction time and longer (see below for comments on estimates of total flux prior to 4 s).

Quantification of cyclic electron flow

The initial re-reduction kinetics of $P700^+$ were obtained by fitting the post-illumination relaxation curves as the sum of three negative exponentials, from which the initial slopes could be calculated to give the

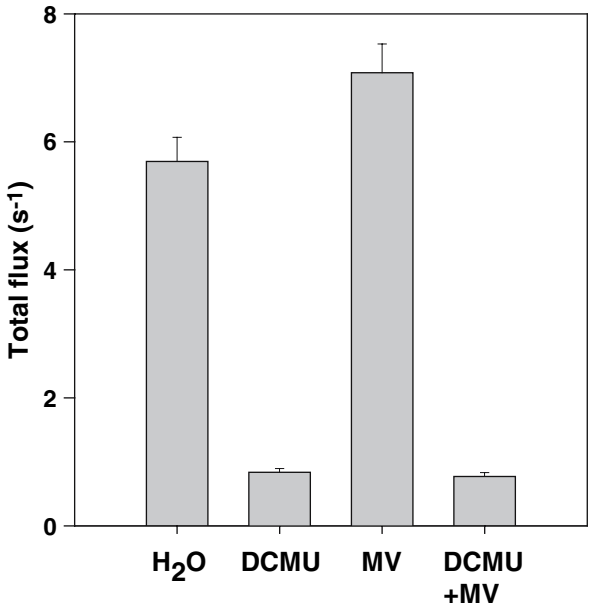

Fig. 8 The total electron flux to $P700^+$ in leaves discs infiltrated with H_2O, DCMU, MV or DCMU + MV at photosynthetic induction time 2 s. Leaves were dark-adapted for 1 h, and then illuminated with red + far-red actinic light for 2 s before measurement of the post-illumination kinetics of $P700^+$. Other conditions as for Fig. 3

total flux of electrons arriving at $P700^+$ immediately before cessation of illumination. The total electron flux, increasing to a maximum at 30 s induction time and decreasing thereafter in H_2O-infiltrated leaf samples, was much diminished in the presence of MV which abolished cyclic electron flow (Fig. 3G). However, the total linear electron flux in the presence of MV did not undergo any significant induction, whereas the total flux in H_2O-infiltrated samples did. Therefore, one cannot simply use the difference between the two fluxes to estimate the cyclic electron flux while photosynthetic induction was in progress. To derive the linear electron flux during photosynthetic induction, we monitored the quantity $(1 - F/F_m')$ which is directly proportional to the linear electron flow through PS II. Interestingly, such a relative measure of linear electron flow through PS II was identical for H_2O- and MV-infiltrated leaf discs at 60 s of photosynthetic induction or longer (Fig. 4). This coincidence allowed us to scale the relative linear flux in H_2O-infiltrated leaf discs in Fig. 4 (open circles) so that, at 60 s, it has the same numerical value as for MV-infiltrated samples in Fig. 3G (open circles), giving curve (b) in Fig. 5A. Then it was possible to obtain the cyclic electron flux (curve (a)) as the difference between the total flux (curve (c)) and the linear flux (curve (b)) during photosynthetic induction in Fig. 5A. The linear electron flux through PS II could consist of electron flow to $NADP^+$ or to O_2 via a Mehler-ascorbate-peroxidase reaction. Both partial linear electron fluxes might undergo induction, but they both occurred in curves (b) and (c) in Fig. 5A, so subtraction cancels both linear partial fluxes, allowing quantification of the cyclic electron flux.

Figure 5B curve (a) shows that the cyclic flux, as a fraction of the total, increased to a maximum of about 68% at 30 s. At the same time the contribution of linear electron flow fell to a minimum, presumably due to its down-regulation by the pH gradient generated by cyclic electron flow (Heber and Walker 1992) and possibly by O_2-dependent electron flow (Schreiber et al. 1995). Subsequently, the cyclic flux declined to about 37% at 90 s.

At long photosynthetic induction times (several minutes), the cyclic electron flux, in our leaf discs under moderately low red + far-red actinic irradiance, declined to a few percent of the total (Fig. 6B). This agrees with the observations of Joliot and Joliot (2006) for moderate green light and those of Laisk et al. (2005). Given the hypothesis that the relative occurrence of linear and cyclic electron flow depends on the rate of electron transfer from Fd^- to $NADP^+$ via ferredoxin-NADP reductase (Joliot and Joliot 2006), we expect that during steady-state photosynthesis under normal conditions, $NADP^+$ is relatively abundant, and readily accepts electrons from Fd^-. Under such conditions, linear electron flow out-competes cyclic flow. On the other hand, in anaerobic (Joët et al. 2002), chilling (Clarke and Johnson 2001) or drought conditions (Golding et al. 2004), carbon assimilation is retarded, cyclic electron flow is increased, and linear electron flow is diminished, as expected.

The cyclic electron flux during early photosynthetic induction was low

On a time scale of minutes, the data of Joliot and Joliot (2006), obtained from the onset phase of P700 photooxidation, revealed that the cyclic flux constitutes about 85% of the total at the earliest time point (about 5 s). In contrast, our earliest time point at 2 s yielded a small cyclic flux (ca. 12% of the total electron flux, Fig. 5 curve (b)). However, since our cyclic flux increased threefold by 4 s, there may not be any serious discrepancy at 4–5 s between the two observations, which were made under different light conditions.

Even our slow cyclic flux at 2 s was almost certainly an *overestimate*. The total flux to $P700^+$ strictly consists of three partial fluxes: a cyclic flux, a PS II linear electron flux and a stromal flux that originated in

stromal reductants feeding electrons into the PQ pool. Simple subtraction of the PS II linear electron flux from the total, therefore, overestimated the cyclic flux, particularly before stromal reductants were depleted by light-induced electron transfer to $NADP^+$ or O_2. Indeed, as seen in Fig. 8 in the combined presence of DCMU (an inhibitor of linear electron flow) and MV (a competitor of cyclic electron flow), the residual electron flux of 0.77 turnovers of each P700 s^{-1} (~13% of the total electron flux) at 2 s was almost certainly due to electron flow from stromal reductants. This stromal flux declined to 0.31 s^{-1} (~3% of the total electron flux) by 90-s illumination (data not shown), presumably due to partial depletion of the pool of stromal reductants.

Poising of cyclic electron flow by electrons from PS II

The fast electron flux with a rate coefficient of 30–50 s^{-1} (depending on the presence or absence of MV), dominated the post-illumination kinetics of $P700^+$ after 30 s actinic light. Its marked sensitivity to MV (Fig. 7F) strongly suggests that it is a cyclic electron flux. Further, this MV-sensitive cyclic electron flow was sensitive to DCMU, which blocks linear electron transfer in PS II. We interpret the DCMU effect on the MV-sensitive component as being due to inhibition of the redox poising of the intersystem electron transport chain. Cyclic electron flow cannot occur if its components are either completely reduced (because there is nowhere for the electrons to go) or completely oxidized (because there are no electrons to cycle) (Whatley 1995; Allen 2003). The red + far-red actinic light used in this study had a component with wavelengths below 700 nm capable of stimulating PS II (Chow and Hope 2004; Hughes et al. 2006); electrons from water oxidation in PS II could then be injected into the cyclic chain to poise it for optimal cyclic flow. In the presence of >30 μM DCMU, however, such poising was prevented, resulting in the loss of not only (1) the MV-resistant fast flux (attributable to linear electron transport from PS II to $P700^+$), but also (2) the MV-sensitive fast flux (attributable to cyclic electron flow) (Fig. 7F).

In this study, we have not addressed the various possible routes of cyclic electron flow around PS I, mediated by (1) the putative ferredoxin-plastoquinone reductase (Bendall and Manasse 1995) as regulated by the *pgr5* gene product (Munekage et al. 2004) and (2) NAD(P)H dehydrogenase (Mi et al. 1995) or the ferredoxin-NADP reductase (Buhkov and Carpentier 2004). Nor have we addressed the possibility that the different post-illumination relaxation phases correspond to (1) populations of PS I with distinct properties (Albertsson 1995), (2) the same enzymes located in different membrane domains (Buhkov et al. 2002), (3) different enzymes mediating different routes (Chow and Hope 2004), or (4) heterogeneity of PS II reaction centres. Instead, we quantified, by subtraction of the linear electron flux from the total flux, a cyclic electron flux which might represent the combined contributions of different routes.

In conclusion, our results show that during photosynthetic induction under moderately low red + far-red light, the rate of cyclic electron transport started from a low value, increased to a maximum of 11–15 turnovers of each P700 s^{-1} (68% of the total electron flux) after about 30 s of illumination, and declined gradually until it was <10% of the total electron flux through PS I in the steady state. Further, we have demonstrated the quantification of the cyclic electron flux with a relatively straightforward method.

Acknowledgements DF is supported in part by the National Natural Science Foundation of China (No. 90302004) and Knowledge Innovation Program of the Chinese Academy of Sciences (KSCX2-SW-109). Partial financial support of this project from an ARC grant DP 0665363 to BJP and WSC is gratefully acknowledged. ABH is grateful for a Visiting Fellowship from RSBS, ANU. We thank Jan Anderson and Tom Wydrzynski for constructive comments on the manuscript.

References

Albertsson P-Å (1995) The structure and function of the chloroplast photosynthetic membrane – a model for the domain organization. Photosynth Res 46:141–149

Arnon DI, Whatley FR, Allen MB (1955) Vitamin K as a cofactor of photosynthetic phosphorylation. Biochim Biophys Acta 16: 607–608

Allen JF (2003) Cyclic, pseudocyclic and noncyclic photophosphorylation: new links in the chain. Trends Plant Sci 8:15–19

Bendall DS, Manasse R (1995) Cyclic photophosphorylation and electron transport. Biochim Biophys Acta 1229:23–38

Buhkov NG, Carpentier R (2004) Alternative Photosystem I-driven electron transport routes: mechanisms and functions. Photosynth Res 82:17–33

Buhkov NG, Egorova E, Carpentier R (2002) Electron flow to Photosystem I from stromal reductants in vivo: the size of the pool of stromal reductants controls the rate of electron donation to both rapidly and slowly reducing Photosystem I units. Planta 215:812–820

Buhkov NG, Weise C, Neimanis S, Heber U (1999) Heat sensitivity of chloroplasts and leaves: Leakage of protons from thylakoids and reversible activation of cyclic electron transport. Photosynth Res 59:81–93

Chow WS, Hope AB (2004) Electron fluxes through photosystem I in cucumber leaf discs probed by far-red light. Photosynth Res 81:77–89

Clarke JE, Johnson GN (2001) In vivo temperature dependence of cyclic and pseudocyclic electron transport in barley. Planta 212:808–816

Cornic G, Buhkov NG, Weise C, Bligny R, Heber U (2000) Flexible coupling between light-dependent electron and vectorial transport in illuminated leaves of C3 plants. Role of photosystem I-dependent proton pumping. Planta 210:468–477

Furbank RT, Jenkins CLD, Hatch MD (1990) C_4 Photosynthesis: quantum requirement, C_4 acid overcycling and Q-cycle involvement. Aust J Plant Physiol 17:1–7

Genty B, Briantais J-M, Baker NR (1989) The relationship between quantum yield of photosynthetic electron transport and quenching of chlorophyll fluorescence. Biochim Biophys Acta 990:87–92

Golding AJ, Finazzi G, Johnson GN (2004) Reduction of the thylakoid electron transport chain by stromal reductants—evidence for activation of cyclic electron transport upon dark adaptation or under drought. Planta 220:356–363

Golding AJ, Joliot P, Johnson GN (2005) Equilibrium between cytochrome *f* and P700 in intact leaves. Biochim Biophys Acta 1706:105–109

Havaux M (1996) Short-term responses of Photosystem I to heat stress. Induction of a PS II-independent electron transport through PS I fed by stromal components. Photosynth Res 47:85–97

Heber U, Walker D (1992) Concerning a dual function of coupled cyclic electron transport in leaves. Plant Physiol 100:1621–1626

Herbert SK, Fork DC, Malkin S (1990) Photoacoustic measurements in vivo of energy storage by cyclic electron flow in algae and higher plants. Plant Physiol 94:926–934

Hughes JL, Smith P, Pace R, Krausz E (2006) Charge separation in photosystem II core complexes induced by 690–730 nm excitation at 1.7 K. Biochim Biophys Acta 1757:841–851

Joët T, Cournac L, Peltier G, Havaux M (2002) Cyclic electron flow around photosystem I in C3 plants. In vivo control by the redox state of chloroplasts and involvement of the NADPH-dehydrogenase complex. Plant Physiol 128:760–769

Johnson GN (2005) Cyclic electron transport in C_3 plants: fact or artefact? J Exp Bot 56:407–416

Joliot P, Joliot A (2002) Cyclic electron transfer in plant leaf. Proc Natl Acad Sci USA 99:10209–10214

Joliot P, Joliot A (2005) Quantification of cyclic and linear flows in plants. Proc Natl Acad Sci USA 102:4913–4919

Joliot P, Joliot A (2006) Cyclic electron flow in C3 plants. Biochim Biophys Acta 1757:362–368

Kramer DM, Avenson TJ, Edwards GE (2004) Dynamic flexibility in the light reactions of photosynthesis governed by both electron and proton transfer reactions. Trends Plant Sci 9:349–357

Laisk A, Eichelmann, Oja V, Peterson RB (2005) Control of cytochrome b_6f at low and high light intensity and cyclic electron transport in leaves. Biochim Biophys Acta 1708:79–90

Maxwell PC, Biggins J (1976) Role of cyclic electron transport in photosynthesis as measured by the photoinduced turnover of P700 in vivo. Biochemistry 15:3975–3981

Mi H, Endo T, Ogawa T, Asada K (1995) Thylakoid membrane-bound pyridine nucleotide dehydrogenase complex mediates cyclic electron transport in the cyanobacteria *Synechocystis* PCC 6803. Plant Cell Physiol 36:661–668

Munekage Y, Hashimoto M, Miyake C, Tomizawa K-I, Endo T, Tasaka M, Shikanai T (2004) Cyclic electron flow around photosystem I is essential for photosynthesis. Nature 429:579–582

Sacksteder CA, Kramer DM (2000) Dark-interval relaxation kinetics (DIRK) of absorbance changes as a quantitative probe of steady-state electron transfer. Photosynth Res 66:145–158

Schreiber U (2004) Pulse-amplitude-modulation (PAM) fluorometry and saturation pulse method: an overview. In: Papageorgiou GC, Govindjee (eds) Advances in photosynthesis and respiration, vol 19, Chlorophyll *a* fluorescence: a signature of photosynthesis. Springer, Dordrecht, The Netherlands, pp 279–319

Schreiber U, Hormann H, Asada K, Neubauer C (1995) O_2-dependent electron flow in spinach chloroplasts: properties and possible regulation of the Mehler-ascorbate-peroxidase cycle. In: Mathis P (ed) Photosynthesis: from light to biosphere, vol II. Kluwer Academic Publishers, Dordrecht, The Netherlands, pp 813–818

Whatley FR (1995) Photosynthesis by isolated chloroplasts: the early work in Berkeley. Photosynth Res 46: 17–26